

# Multimaterial Coatings Design via Exhaustive Search for Gravitational Wave Detectors

V. Pierro,<sup>1, 2, \*</sup> V. Fiumara,<sup>3, 2</sup> F. Chiadini,<sup>4, 2</sup> V. Granata,<sup>5, 2</sup> C. Di Giorgio,<sup>6, 2</sup> O. Durante,<sup>6, 2</sup> J. Neilson,<sup>1, 2</sup> R. Fittipaldi,<sup>5, 2</sup> G. Carapella,<sup>6, 2</sup> F. Bobba,<sup>6, 2</sup> and I. M. Pinto<sup>1, 2, 7</sup>

<sup>1</sup>*Dipartimento di Ingegneria, Università del Sannio, I-82100 Benevento, Italy.*

<sup>2</sup>*INFN, Sezione di Napoli Gruppo Collegato di Salerno,*

*Complesso Universitario di Monte S. Angelo, I-80126 Napoli, Italy.*

<sup>3</sup>*Scuola di Ingegneria, Università della Basilicata, I-85100 Potenza, Italy.*

<sup>4</sup>*Dipartimento di Ingegneria Industriale DIIN, Università di Salerno, I-84084 Fisciano, Salerno, Italy.*

<sup>5</sup>*CNR-SPIN, c/o Università di Salerno, I-84084 Fisciano, Salerno, Italy.*

<sup>6</sup>*Dipartimento di Fisica "E.R. Caianiello", Università di Salerno, I-84084 Fisciano, Salerno, Italy.*

<sup>7</sup>*Museo Storico della Fisica e Centro Studi e Ricerche "Enrico Fermi", I-00184 Roma, Italy.*

In this work we analyze coatings for gravitational wave detector mirrors obtained by sequencing dielectric layers, with fixed thicknesses, made of three different materials (ternary sequences). Two materials are chosen non-dissipative, i.e. are the standard oxides used in gravitational wave detector coatings technology, the third is a dissipative material.

We use the methodology of the exhaustive smart search in the space of sequences to find out the coating design with minimal thermal noise satisfying suitable constraints on transmittance and absorbance. This search has a combinatorial computational complexity and is carried out with a backtracking algorithm.

The results obtained show that these ternary sequences can satisfy the optical transmittance and absorbance constraints requested by the mirrors of gravitational wave interferometers, reducing the thermal noise of the coating compared to the standard configuration made of two non-dissipative materials.

In all the examined cases the dissipative material is positioned on the bottom of the optimal sequence of the coating layers, close to the substrate. Furthermore, the optimal designs are robust with respect to the uncertainty of the extinction coefficient and have spectral behaviors similar to the quarter wave coatings.

Finally, the possibility of further improving performance in terms of thermal noise is demonstrated by considering sequences made of non-quarter wavelength layers.

**Keywords:** Thin Films, Dielectric Mirrors, Gravitational Wave Detectors

## I. INTRODUCTION

The thermal noise reduction of the coatings of the test mass mirrors in the gravitational wave detectors [1, 2] is an important achievement to be obtained in order to increase the sensitivity in the frequency band relevant for astrophysical source detection [3–6]. For this purpose, some gravitational wave antennas experiments have chosen to lower the temperature until reaching cryogenic temperatures [7]. The challenge to be faced is to design coatings with very high reflectivity, extremely low absorption and minimal thermal noise. A possible well established strategy (see Chapt. 6 in [8]) consists in using binary coating made of two amorphous materials with high and low refractive index. In particular, the coatings which are used in both LIGO and Virgo interferometers are made of silica ( $\text{SiO}_2$ ) and titania doped tantalum ( $\text{Ti}:\text{Ta}_2\text{O}_5$ ) deposited on bulk silica end test mass [9]. The extinction coefficient of both  $\text{SiO}_2$  and  $\text{Ti}:\text{Ta}_2\text{O}_5$  is negligible at the operating wavelength of  $\lambda_0 = 1064$  nm. The standard design consists in alternating layers

of these materials which are quarter-wave at  $\lambda_0$ . Alternative designs of binary coating with non quarter-wave layers have been proposed in order to reduce the thermal noise [10–12].

In a recent paper we faced the general optimization problem of a binary coating consisting of non-dissipative materials, by using a multi-objective approach [13]. We showed that the layer thickness optimization, without any a priori hypothesis, lead to a reduction of thermal noise which can not exceed  $\sim 17\%$  of the standard design. However, further reduction of thermal noise is necessary to increase the visibility distance of gravitational wave detectors.

In this connection, the possibility of using some additional materials also with a not negligible extinction coefficient has been investigated in the last years [14–16]. Multimaterial designs have been proposed where the coating consists in a stack of different half-wave doublets, which are bilayers made of two low and high refractive index materials with quarter-wave optical length. Three material coatings are considered in [17] where amorphous Si (a-Si) is proposed as the third material. In particular a sequence of  $\text{Ti}:\text{Ta}_2\text{O}_5/\text{SiO}_2$  and a-Si/SiO<sub>2</sub> doublets is showed to satisfy the optical constraints (very low transmittance and absorption) with a significant reduction of

\* Corresponding author: pierro@unisannio.it

thermal noise. This geometry agrees with the simplified theory in [14] that suggests the possibility of using dissipative layers at the end of the coating structure, where the field intensity is lower. However, the solution of optimization problem for quarter-wave layers three material coatings has not be definitively established. In particular a rigorous proof of the general accepted idea that dissipative material should be deposited in the terminal part of the coating has never been showed.

In this paper we face the problem of finding out the best performing sequence of quarter-wave layers of three materials giving a coating satisfying the optical constraints with the lowest thermal noise.

It is worth noting that in the case of three materials the optimization without any *a priori* hypotheses, neither on the sequence nor on the thickness of the layers, turns out to be computationally demanding. As a consequence, as a first approach to this general optimization problem, we face the problem of sequence optimization with fixed layer thicknesses. Specifically, we focus on the problem of finding the optimal sequence of quarter-wave layers, which minimizes thermal noise, satisfying the following two constraints: transmittance less than 6 parts per million (henceforth ppm) and absorbance less than 1 ppm.

To solve the above mentioned problem we propose to carry out an exhaustive search in the sequence space, i.e. to examine all the coating designs made of all possible sequences of materials. This is a typical constraint satisfaction problem [18, 19], which has a combinatorial complexity that explodes exponentially with the number of layers [20]. To face this difficulty we developed a smart code that using a backtracking approach (see pag. 74 [18]) reduces the number of matrix products to be computed in order to evaluate the transmittance and absorbance for all sequences.

Following [14] we consider a set of materials constituted by  $\text{SiO}_2$ ,  $\text{Ti}:\text{Ta}_2\text{O}_5$  and a hypothetical third material with a moderately high extinction coefficient. The geometry and the potential benefit of optimized three material coatings are shown by varying the characteristics of the hypothetical material. In particular, we assume that the third hypothetical material can belong to two possible categories of materials. For the first category (indicated with MA) we assume that the refractive index is similar to doped tantalum but with lower mechanical losses. For the second category (indicated with MB) we assume that the refractive index is higher than that of doped tantalum, but with comparable mechanical losses.

We note that the two categories of materials have characteristics similar to two particularly promising materials examined in the literature: silicon nitride [21, 22] and amorphous silicon [23]. Furthermore, recent studies [24, 25] have shown that, in principle, materials belonging to the MA category could be made by the nano-layering technique.

Finally, we show that a further reduction of thermal noise can be obtained by using three material coatings

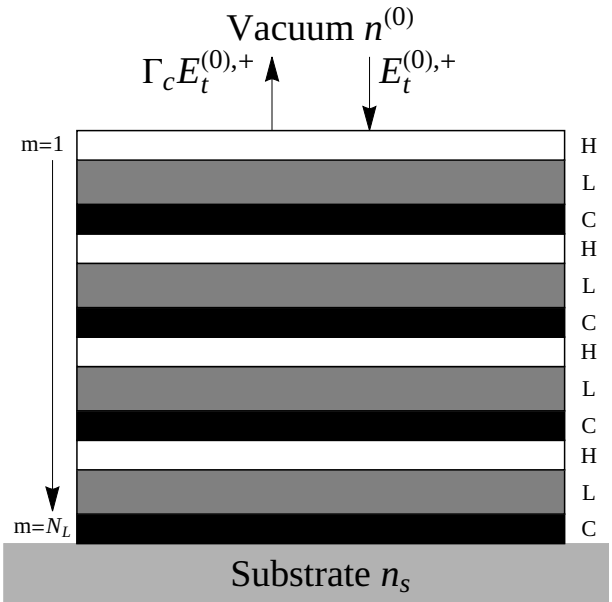


FIG. 1. An illustration of a ternary coating made of H (white), L (gray) and C-type (black) materials. The layers are numbered starting from the top ( $m = 1$ ), where the incident field (i.e. a normal monochromatic waves impinging from the vacuum) and the reflected field are indicated. The half space on the top is the vacuum with refractive index  $n^{(0)}$ , the coating is deposited on a substrate with refractive index  $n_s$ . The last layer, which is in contact with substrate, has number  $m = N_L$  where  $N_L$  is the number of deposited layers.

with non quarter-wave layers.

## II. THE COATING MODEL

In this section we report the complete model of a multi-material coating, referring to [8] for a comprehensive introduction to the topic. In particular, we introduce the optical model based on the transmission matrix formalism [26] and the simplified thermal noise model of the coating [6].

In the following an  $\exp(i 2\pi f_0 t)$  dependence on time  $t$  is implicit, where  $f_0$  is the laser (operating) frequency and  $i$  is the imaginary unit.

### A. Coating optical model

The optical response of a multilayer coating can be computed from the characteristic matrix

$$\mathbf{T} = \mathbf{T}_1 \cdot \dots \cdot \mathbf{T}_m \cdot \dots \cdot \mathbf{T}_{N_L} \quad (1)$$

where  $N_L$  is the total number of layers numbered from the vacuum to the substrate as illustrated in Fig. 1, and  $\mathbf{T}_m$  is the transmission matrix of the  $m$ -th layer in the

case of normal incidence [8]:

$$\mathbf{T}_m = \begin{bmatrix} \cos(\psi_m) & \imath(n^{(m)})^{-1} \sin(\psi_m) \\ \imath n^{(m)} \sin(\psi_m) & \cos(\psi_m) \end{bmatrix}, \quad (2)$$

where

$$\psi_m = \frac{2\pi}{\lambda_0} n^{(m)} d_m, \quad (3)$$

$\lambda_0$  and  $d_m$  being the free space wavelength and the layer thickness, respectively, and

$$n^{(m)} = n_r^{(m)} - \imath\kappa^{(m)}. \quad (4)$$

In the following we refer to  $n^{(m)}$  as the complex refractive index,  $n_r^{(m)}$  as the refractive index and  $\kappa^{(m)}$  as the extinction coefficient.

The coating is placed between two homogeneous non dissipative dielectric half-spaces with refractive indexes  $n^{(0)}$  and  $n_s$ , respectively (see Fig. 1). The bottom half-space (with refractive index  $n_s$ ) is the substrate, while the uppermost is the vacuum (with refractive index  $n^{(0)}$ ). Let a monochromatic plane wave impinge normally on the coating from the vacuum.

The effective complex refractive index of the whole multilayer structure  $n_c$  is,

$$n_c = \frac{T_{21} + n_s T_{22}}{T_{11} + n_s T_{12}}, \quad (5)$$

that can be used to compute the reflection coefficient  $\Gamma_c$  at the vacuum/coating interface :

$$\Gamma_c = \frac{n^{(0)} - n_c}{n^{(0)} + n_c}. \quad (6)$$

The transmittance at the vacuum/coating interface is

$$\tau_p = \frac{\mathcal{P}_{in}}{\mathcal{P}^+} = 1 - |\Gamma_c|^2 \quad (7)$$

where  $\mathcal{P}_{in}$  is the power density flowing into the coating at the first interface (vacuum/coating) and  $\mathcal{P}^+$  is the power incident from the vacuum,

$$\mathcal{P}^+ = n^{(0)} \frac{1}{2Z_0} |E_t^{(0),+}|^2 \quad (8)$$

where  $E_t^{(0),+}$  is the incident transverse electrical field at the vacuum/coating interface and  $Z_0 = \sqrt{\mu_0/\epsilon_0}$  is the characteristic impedance of the vacuum.

The average power density dissipated within the coating can be computed as the difference between  $\mathcal{P}_{in}$  and the power density flowing into the substrate (last interface)  $\mathcal{P}_{out}$ . This last can be computed as follow

$$\mathcal{P}_{out} = \frac{1}{2} \operatorname{Re}(E_t^{(N_L)} H_t^{(N_L)*}) \quad (9)$$

where  $E_t^{(N_L)}$  and  $H_t^{(N_L)}$  are total transverse electric and magnetic fields at the last interface, and  $\operatorname{Re}(\cdot)$  indicates the real part of complex number. The complex amplitude  $E_t^{(N_L)}$  and  $Z_0 H_t^{(N_L)}$  are obtained from  $E_t^{(0)} = E_t^{(0),+}(1 + \Gamma_c)$  and  $Z_0 H_t^{(0)} = n^{(0)} E_t^{(0),+}(1 - \Gamma_c)$  using the formula

$$\begin{bmatrix} E_t^{(N_L)} \\ Z_0 H_t^{(N_L)} \end{bmatrix} = \mathbf{T}^{-1} \begin{bmatrix} E_t^{(0)} \\ Z_0 H_t^{(0)} \end{bmatrix}. \quad (10)$$

From the above the coating absorbance is

$$\mathcal{A} = (\mathcal{P}_{in} - \mathcal{P}_{out})/\mathcal{P}^+ \quad (11)$$

and the transmittance at the coating/substrate interface (i.e. the *normalized* transmitted power in the substrate) is

$$\tau_s = \mathcal{P}_{out}/\mathcal{P}^+. \quad (12)$$

From the Poynting theorem we have  $\tau_p = \mathcal{A} + \tau_s$ . If all the materials have negligible extinction coefficient  $\mathcal{A} = 0$ . In general being  $\tau_s \geq 0$  we have that  $\tau_p \geq \mathcal{A}$ , in other words a constraint on the power transmittance  $\tau_p$  is also a constraint on the power absorbance.

## B. Coating thermal noise model

The power spectral density of coating thermal noise  $S_{coat}^B(f)$  is proportional to the mechanical loss angle  $\phi_c$

$$S_{coat}^B(f) \propto \frac{T}{wf} \phi_c \quad (13)$$

where  $f$  is the frequency,  $T$  is the (absolute) temperature,  $w$  is the (assumed Gaussian) laser-beam waist. The mechanical loss angle for the whole coating is [6]

$$\phi_c = \sum_{m=1}^{N_L} \eta_m d_m \quad (14)$$

where the specific loss angle is

$$\eta_m = \frac{1}{\sqrt{\pi}w} \phi_m \left( \frac{Y_m}{Y_s} + \frac{Y_s}{Y_m} \right) \quad (15)$$

$\phi_m$  and  $Y_m$  being the mechanical loss angle and the Young's modulus of the  $m$ -th layer, respectively.

According to eq. (13), increasing the beam-width  $w$  and lowering the temperature  $T$  results in a reduction of coating noise [6]. Using wider non Gaussian beams (e.g., higher order Gauss-Laguerre) is another option, also being currently investigated [27]. Decreasing the temperature  $T$  works for materials that does not exhibit mechanical loss peaks at the (cryo) temperatures of interest [28]. Current research is accordingly focused on finding (synthesizing and optimizing) *better* materials featuring low optical absorption and scattering losses, low mechanical losses down to cryo temperatures, and high optical

contrast (allowing fewer layers to achieve a prescribed transmittance, resulting into thinner coatings and lower noise). In this paper we focus on reducing the coating loss angle  $\phi_c$  by optimizing coating architecture consisting in a sequence of layers of three materials.

### III. EXHAUSTIVE SEARCH FOR TERNARY COATING

Recently, multimaterial coating have been proposed for gravitational wave detectors [14], [15], [17]. In particular three material coatings are considered in [17] where a sequence of two different quarter wavelength (henceforth QW) binary coatings ( $\text{Ti}:\text{Ta}_2\text{O}_5/\text{SiO}_2$  followed by  $\text{a-Si/SiO}_2$ ) is proposed. This geometry agrees with the simplified theory made in [14] that suggests the possibility of using dissipative layers at the end of the coating structure (i.e. near to the substrate), where the field intensity is lower.

However, a rigorous proof of the general accepted idea that dissipative material should be deposited in the part of the coating closer to the substrate has been never showed. In this paper we face this problem following an exhaustive search approach with the goal of selecting the best performing sequence of QW layers of three materials having  $\tau_p < 6$  ppm and  $\mathcal{A} < 1$  ppm, and exhibiting the lowest thermal noise.

#### A. Hypothetical materials

In this section, following [14], we consider two hypothetical materials MA and MB. The material MA is supposed to have the same refractive index of Ti-doped tantalum and a lower loss angle, while the material MB is supposed to have the same loss angle and higher refractive index than Ti-doped tantalum. For both materials we consider values of the extinction coefficient ranging from  $10^{-7}$  to  $10^{-4}$ . The physical parameters of all used materials are reported in Table I.

In the following, two ternary coatings are analyzed: the MA-type coating where the materials are  $\text{SiO}_2/\text{Ti}:\text{Ta}_2\text{O}_5/\text{MA}$ , and the MB-type coating made of  $\text{SiO}_2/\text{Ti}:\text{Ta}_2\text{O}_5/\text{MB}$ . For both cases the three materials in the coatings are labeled by the symbols H, L and C. The symbols H and L refer to high (titania doped tantalum) and low (silica) refractive index materials with negligible extinction coefficient. The symbol C refers to the dissipative material (MA or MB).

#### B. Single quarter wavelength layer search

The single layer search consists in the performance evaluation of all coating configurations made of a sequence of the three material H, L and C. All layer thicknesses are quarter wave at the operating wavelength

Property	$\text{SiO}_2$	$\text{Ti}:\text{Ta}_2\text{O}_5$	MA	MB
$n_r$	1.45	2.1	2.1	3.0
$\kappa$	$10^{-11}$	$2 \times 10^{-8}$	$y \times 10^{-7}$	$y \times 10^{-7}$
$Y$	72 GPa	140 GPa	100 GPa	100 GPa
$\phi$	$5.0 \times 10^{-5}$	$3.76 \times 10^{-4}$	$10^{-4}$	$3.76 \times 10^{-4}$
$dn_r/d\lambda$ [nm $^{-1}$ ]	$-1.2 \times 10^{-5}$	$-4.9 \times 10^{-5}$	$-3.8 \times 10^{-5}$	$-4.26 \times 10^{-4}$

TABLE I. Physical parameters of coating and substrate materials used in simulations, we assume temperature  $T = 300\text{K}$  and free space wavelength  $\lambda_0 = 1064$  nm. The meaning of symbol is the following:  $n_r$  is the refractive index,  $\kappa$  the extinction coefficient,  $Y$  the Young coefficient,  $\phi$  the specific mechanical loss and  $dn_r/d\lambda$  the chromatic dispersion. The variable  $y$  in the extinction coefficient takes the following values  $y = 1, 10, 10^2, 10^3$ .

$\lambda_0 = 1064$  nm. In all considered sequences two adjacent layers are constituted by different materials.

Let us introduce the ensemble of the QW transmission matrix of the considered materials  $\Omega_T = \{\mathbf{T}_H, \mathbf{T}_L, \mathbf{T}_C\}$ .

Each sequence, consisting of  $N_L$  layers, is characterized by the transmission matrix:

$$\mathbf{T} = \mathbf{T}_1 \cdot \dots \cdot \mathbf{T}_m \cdot \dots \cdot \mathbf{T}_{N_L} \quad (16)$$

where  $\mathbf{T}_m \in \Omega_T$  is the  $m$ -th layer matrix and  $\mathbf{T}_m \neq \mathbf{T}_{m+1}$ . For all layer sequences we compute the matrix (16) giving the transmittance and the absorbance by following the procedure described in Sect. II A.

In order to compute the thermal noise of the three material coatings we introduce the normalized specific loss angles  $\gamma_H$ ,  $\gamma_L$  and  $\gamma_C$ :

$$\gamma_H = \frac{\eta_H}{\eta_L} = \frac{\phi_H}{\phi_L} \left( \frac{Y_H}{Y_s} + \frac{Y_s}{Y_H} \right) \left( \frac{Y_L}{Y_s} + \frac{Y_s}{Y_L} \right)^{-1} \quad (17)$$

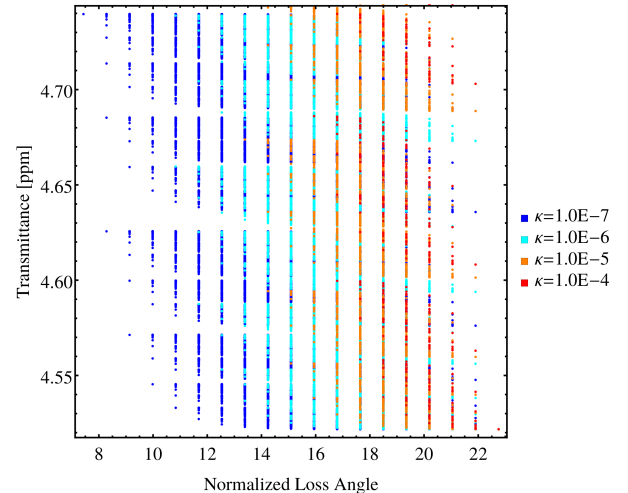


FIG. 2. In the figure we display MA type solutions meeting both the conditions  $\tau_p \leq 6$  ppm and  $\mathcal{A} \leq 1$  ppm in the transmittance mechanical-loss plane. The legend indicates the value of extinction coefficient  $\kappa$  used to obtain the solutions. The number of layers is  $N_L = 36$ , below this value for MA-type coatings no solution can be found.

$$\gamma_C = \frac{\eta_C}{\eta_L} = \frac{\phi_C}{\phi_L} \left( \frac{Y_C}{Y_s} + \frac{Y_s}{Y_C} \right) \left( \frac{Y_L}{Y_s} + \frac{Y_s}{Y_L} \right)^{-1} \quad (18)$$

where  $\phi_L$ ,  $\phi_H$  and  $\phi_C$  are the specific mechanical loss coefficients (see Table I for numerical values at room temperature) and obviously  $\gamma_L = 1$ . Let us define the normalized coating loss angle  $\bar{\phi}_c = \phi_c/(\lambda_0 \eta_L)$  which, using the above defined coefficients, can be written

$$\bar{\phi}_c = N_l \bar{d}_L + N_h \gamma_H \bar{d}_H + N_c \gamma_C \bar{d}_C \quad (19)$$

where  $N_l$ ,  $N_h$  and  $N_c$  are the number of layers made of L, H, and C materials respectively. Furthermore  $\bar{d}_L = 0.25 \text{ Re}(n_L)^{-1}$ ,  $\bar{d}_H = 0.25 \text{ Re}(n_H)^{-1}$  and  $\bar{d}_C = 0.25 \text{ Re}(n_C)^{-1}$  are the normalized QW layer thicknesses.

We developed a Fortran code that assesses the performance of all possible sequences in terms of coating transmittance, absorbance and normalized loss angle. The number of sequences to be evaluated is  $\mathcal{N}_L = 3 \cdot 2^{N_L-1}$  (see Appendix). In view of the high value of  $\mathcal{N}_L$  a simple code, computing the transmission matrix in (16) for each sequence and then evaluating the performances, is too slow in terms of CPU time. In this connection we have implemented a smart code that using a backtracking approach reduces the number of matrix products to be computed. This code allows the inspection [29] of the space of the sequences up to  $N_L \sim 40$ .

In the following the results of ternary coatings will be compared with the *reference coating* made of  $N_L = 36$  QW layers of alternating titania doped tantalum and silica, which is currently used in Virgo/LIGO gravitational wave detectors.

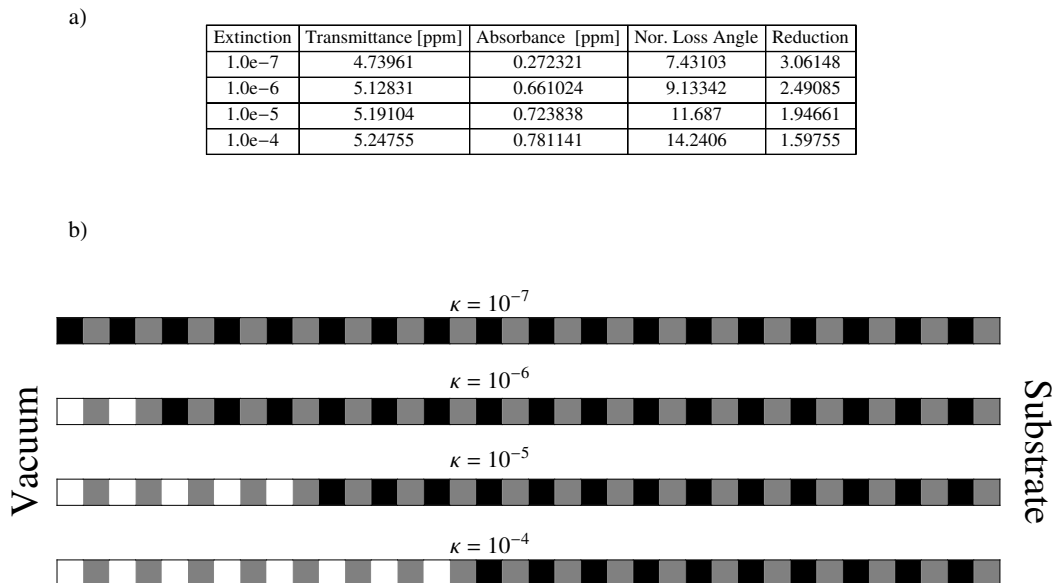


FIG. 3. In the part a) we report the values of transmittance, absorbance and normalized loss angle for the best performing sequences. In the leftmost column the reduction factor of coating loss angle with respect to the standard reference solution (i.e.  $\bar{\phi}_c = 22.75$ ) is reported. In the part b) of the figure we display MA type best solutions satisfying both the conditions  $\tau_p \leq 6$  ppm and  $\mathcal{A} \leq 1$  ppm. The legend indicate the value of extinction coefficient  $\kappa$  used to obtain the solutions, dissipative material (C) is black, low index material (L) is gray and high index material (H) is white.

with integer  $4 \leq s \leq 7$ ) for the extinction coefficient of the material C, and consider all the layers having a QW thickness at  $\lambda_0 = 1064$  nm.

### 1. Results for MA-type coating

In this section we report the performance evaluation of the MA-type coating. We use the values  $\kappa = 10^{-s}$ , (

In Fig. 2 we display  $\tau_p$  and  $\bar{\phi}_c$  for all sequences satisfying the transmittance and the absorbance constraints (i.e.  $\tau_p \leq 6$  ppm and  $\mathcal{A} \leq 1$  ppm) for  $N_L = 36$  and different values of extinction coefficient  $\kappa$ .

In view of the equality  $\text{Re}(n_C) = \text{Re}(n_H)$  there are no sequences satisfying the constraints for  $N_L < 36$ . In fact this is the number of layers of the *reference* QW coating and below this number the  $\tau_p$  constraint is violated.

For low extinction coefficient, it is convenient to substitute in the reference QW design all H-type materials (high loss angle) with a C-type material that in the MA-type material case has a low specific loss angle.

Increasing the optical loss  $\kappa$  some solution is forbidden because of the violation of absorbance constraint. This is further elucidated in Fig. 3b where the schematics of the best coating design are reported. These schematics are displayed as a sequence of colors black, gray and white for C, L and H-type materials, respectively. In the table in Fig. 3a we report the numerical values of the transmittance, absorbance, normalized loss angle  $\bar{\phi}_c$  and the reduction factor for the optimal sequences. The best coating design are those for which the normalized noise is minimal. In the particular case of solutions with the same loss angle, the solution with the minimal absorbance is considered as the best.

It is worth to note that all optimal solutions consists in a sequence of doublets (HL and CL), where the doublets containing non-dissipative material are placed on the top of the coating. Moreover, increasing the extinction coefficient, the number of doublets with dissipative material decreases. The reduction factor of the coating loss angle with respect to the standard reference solution is a decreasing function of the extinction coefficient, ranging from about 3 to about 1.6.

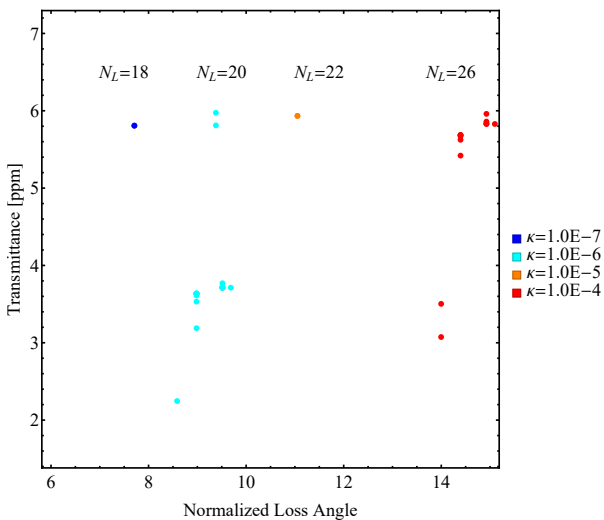


FIG. 4. In the figure we display MB-type solutions meeting both the conditions  $\tau_p \leq 6$  ppm and  $\mathcal{A} \leq 1$  ppm in the transmittance-mechanical-loss plane. The legend indicates the value of extinction coefficient  $\kappa$  used to obtain the solutions. The number of layers change as  $\kappa$  is modified according the value reported in figure.

## 2. Results for MB-type coating

In this subsection we report the performance evaluation of the MB-type coating. As for the MA material, we use the values  $\kappa = 10^{-s}$ , (with integer  $4 \leq s \leq 7$ ) for the extinction coefficient of the material C, and consider all the layers having a quarter wavelength thickness at  $\lambda_0 = 1064$  nm.

In the Fig. 4, for different values of  $\kappa$ , we display  $\tau_p$  and  $\bar{\phi}_c$  for the sequences satisfying the transmittance and the absorbance constraints (i.e.  $\tau_p \leq 6$  ppm and  $\mathcal{A} \leq 1$  ppm). In particular for each value of  $\kappa$  we display only the solutions with minimal  $N_L$ , that have the best performance in terms of loss angle.

In view of the inequality  $\text{Re}(n_C) > \text{Re}(n_H)$  there are solutions satisfying the transmittance and the absorbance constraints with  $N_L < 36$ . Moreover, the minimal value of  $N_L$  is a monotone function of the extinction coefficient. Due to the MB specific loss angle  $\phi$  greater than the MA one, the MB solutions, despite having fewer layers, exhibit a total coating loss angle  $\bar{\phi}_c$  similar to that of MA-type coating.

As for the MA-type coating all optimal solutions consists in a sequence of doublets (HL and CL), where the doublets containing non-dissipative material are placed on the top of the coating. This is elucidated in Fig. 5b where the schematics of the optimal sequences are displayed. The numerical values of the transmittance, absorbance, normalized loss angle  $\bar{\phi}_c$  and the reduction factor for the optimal sequences are displayed in Fig. 5a. Also in this case the reduction factor is a decreasing function of the extinction factor, with values similar to the MA case.

## C. Spectral dependence and robustness

In this section we analyze the properties of the transmittance spectra of the optimal MA and MB design described above. Moreover, we study the robustness of the designs with respect to the uncertainty of the extinction coefficient value. The transmittance spectra have been computed taking into account the chromatic dispersion. We considered the refractive index as a linear function of the wavelength in the neighborhood of the operating wavelength ( $\lambda_0 = 1064$  nm):

$$n_r(\lambda) = n_r(\lambda_0) + \left. \frac{dn_r}{d\lambda} \right|_{\lambda_0} (\lambda - \lambda_0). \quad (20)$$

The values of the derivative in eq. (20) are reported in Table I (see [30]). The data for the MA and MB materials refer to silicon nitride and amorphous silicon, respectively.

In the case of MA-type coating, because the dissipative material has the refractive index equal to the Ti-doped tantalum, it is not surprising that the transmittance spectrum is very close to the one of the quarter-wavelength

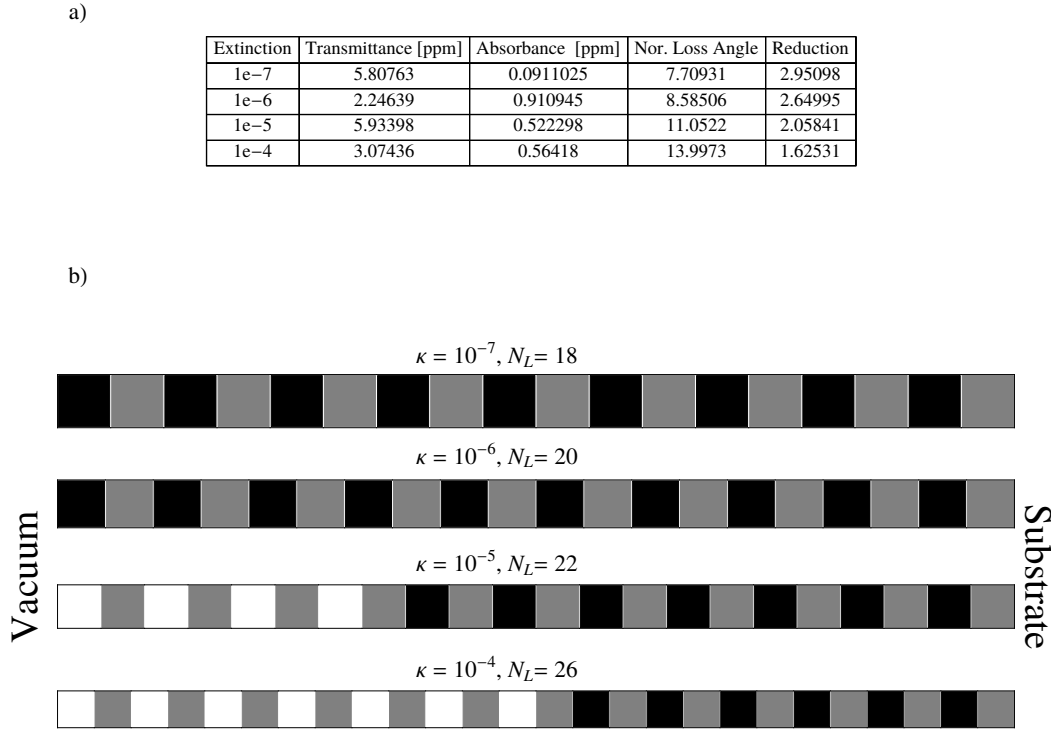


FIG. 5. In the part a) we report the values of transmittance, absorbance and normalized loss angle for the best performing sequences. In the leftmost column the reduction factor of coating loss angle with respect to the standard reference solution (i.e.  $\bar{\phi}_c = 22.75$ ) is reported. In the part b) of the figure we display MB type best solutions satisfying both the conditions  $\tau_p \leq 6$  ppm and  $\mathcal{A} \leq 1$  ppm. The legend indicate the value of extinction coefficient  $\kappa$  used to obtain the solutions, dissipative material (C) is black, low index material (L) is gray and high index material (H) is white.

reference design. This is shown in Fig. 6a where the transmittance spectra for both designs are reported for the case  $\kappa = 10^{-5}$ . A similar behaviour can be observed considering different values of  $\kappa$ .

In the case of MB-type coating the dissipative material has refractive index which significantly differs from the refractive index of the Ti-doped tantalum. Accordingly the transmittance spectra of MB-type coating and the reference design are different. This can be observed in Fig. 7a and Fig. 8a, where the transmittance spectra of both designs are reported for the case  $\kappa = 10^{-5}$  and  $\kappa = 10^{-4}$ , respectively. However, for both MA and MB-type coatings the spectral characteristics of the transmittance should match the transmittance requirements in the entire (very narrow) operating wavelength band of the laser interferometer.

We further analyze the effect of the possible uncertainty of the value of the extinction coefficient  $\kappa$  used for simulations. To this end, we consider two possible causes of this variability, a non-negligible uncertainty in the measurement of the extinction coefficient and some instability in the deposition procedure. In the last case,

all the dissipative layers have different values of  $\kappa$  that is treated as a random variable.

The robustness of the MA-type coating optimal configuration obtained for the nominal value  $\kappa = 10^{-5}$  is illustrated in Fig. 6b considering  $\kappa$  as a random variable uniformly distributed in the range  $[0.5 \times 10^{-5}, 1.5 \times 10^{-5}]$  for both uncertainties. In particular, the distributions of transmittance and absorbance, computed by considering  $10^5$  realizations, are reported on the left for the uncertainty of the measure of  $\kappa$  and on the right for uncertainty due to instability in the deposition procedure. Figures 7b and 8b show the same properties of Fig. 6b but for MB-type coating optimal configurations obtained for the nominal value  $\kappa = 10^{-5}$  and  $\kappa = 10^{-4}$ , respectively. In these cases the realizations have been obtained considering  $\kappa$  as a random variable uniformly distributed in the ranges  $[0.5 \times 10^{-5}, 1.5 \times 10^{-5}]$  and  $[0.5 \times 10^{-4}, 1.5 \times 10^{-4}]$ , respectively.

It can be noted that all optimal configurations are robust concerning the uncertainty of the extinction coefficient of the dissipative material, i.e. almost all realizations are below the design constraints. It can be

$\kappa$	Design	$\tau_p$ [ppm]	$\mathcal{A}$ [ppm]	nor. loss angle	reduction
$10^{-5}$	5(HL) + 16(CL)	4.80	0.98	10.93	2.08
$10^{-4}$	9(HL) + 12(CL)	4.64	0.76	13.20	1.72

TABLE II. MA - type doublets search with non quarter wave layer thicknesses. The less noisy material (indicated with L) has a thickness  $\delta_L = 4/3\bar{d}_L$ .

$\kappa$	Design	$\tau_p$ [ppm]	$\mathcal{A}$ [ppm]	nor. loss angle	reduction
$10^{-5}$	5(HL) + 11(CL)	2.86	0.67	10.50	2.17
$10^{-4}$	9(HL) + 9(CL)	2.96	0.82	12.52	1.82

TABLE III. MB - type doublets search with non quarter wave layer thicknesses. The less noisy material (indicated with L) has a thickness  $\delta_L = 3/2\bar{d}_L$ .

noted that a small number of realizations in Fig. 7b exhibits a transmittance exceeding the constraint value (6 ppm). This is because in the case of MB-type coating the optimal configuration obtained for the nominal value  $\kappa = 10^{-5}$  exhibits a transmittance of about 5.93 ppm which is very close to the constraint limiting value.

#### D. Doublets search

In the previous paragraph we showed that the optimal design of a ternary coating consists of a cascade of two sequences of doublets with optical length equal to  $\lambda_0/2$ , where the layers are supposed quarter wave thick.

In this section we will explore the possibility of improving the coating performance (in terms of noise) considering a cascade of  $\lambda_0/2$  doublets in which the two component layers do not have the same optical length.

In principle, the search for optimal design could be done using the single layer search approach with optical length of the single layer equal to  $\lambda_0/(4m)$  for integer  $m \geq 2$  and removing the hypothesis that adjacent layers are different. This approach for the simplest case  $m = 2$  requires an excessive computational burden, that with the conventional calculation resources is intractable (see Appendix). Nevertheless, in order to show the possibility of noise reduction using not  $\lambda_0/4$  layers, it is not necessary to find the optimum design by an exhaustive search with single layers.

In this connection we consider two type of  $\lambda_0/2$  doublets (i.e. HL and CL), where the less noisy material has a normalized thickness  $\delta_L \geq \bar{d}_L$ , and perform an exhaustive search on all possible combinations of these two doublets.

Let us introduce the ensemble of the transmission matrices of the considered  $\lambda_0/2$  doublets  $\Omega_T = \{\mathbf{T}_H \cdot \mathbf{T}_L, \mathbf{T}_C \cdot \mathbf{T}_L\}$ , here  $\mathbf{T}_H$ ,  $\mathbf{T}_L$  and  $\mathbf{T}_C$  are, in general, non-QW transmission matrices.

Each sequence, consisting of  $N_D$  doublets, have the

following transmission matrix:

$$\mathbf{T} = \mathbf{T}_1 \cdot \dots \cdot \mathbf{T}_m \cdot \dots \cdot \mathbf{T}_{N_D} \quad (21)$$

where  $\mathbf{T}_m \in \Omega_T$  is the  $m$ -th doublet matrix. For any sequence we compute the transmission matrix (21), than the transmittance and the absorbance by following the method in section II.

The results obtained using  $\delta_L = 4/3\bar{d}_L$  for MA and  $\delta_L = 3/2\bar{d}_L$  for MB, are displayed in Table II and III respectively. It can be seen that the search finds solutions with a higher number of doublets but with a reduced coating loss angle with respect to the QW single layer search. It is worth to note that the possibility of reducing noise (below the QW search) depends on the choice of  $\delta_L$ . In fact  $\delta_L = 3/2\bar{d}_L$  does not produce a noise reduction for the MA case.

These results indicate that the optimal design with three materials should be obtained by performing a thicknesses optimization.

This optimal solution cannot be found by an exhaustive search on all possible thickness values since this computational burden is out of the reach of current computer (see Appendix).

## IV. CONCLUSION

In this article we have addressed the problem of optimizing a coating consisting of layers of three materials (ternary coating) with high reflectivity and low thermal noise. This device could be used to make dielectric mirrors necessary for the new-generation of gravitational wave detectors. To date, coatings for gravitational wave detection are made using two materials with very low optical losses ( $\text{SiO}_2$  and  $\text{Ti}:\text{Ta}_2\text{O}_5$ ). In the present article we study the possibility that a third material with higher optical losses is used in addition, in order to improve the coating performances. As a third material we have considered a hypothetical material that can belong to two possible categories. For the first category we assume that the refractive index is similar to Ti-doped tantalum but with lower mechanical losses, for the second category we assume that the refractive index is higher than that of Ti-doped tantalum, but with comparable mechanical losses.

The methodology used to obtain the design of the mirrors was to evaluate the performances of all possible combinations of materials (*exhaustive search*), with fixed layer thicknesses. An *exhaustive* search without any a priori hypotheses, neither on the sequence nor on the thickness of the layers, due to the combinatorial complexity of the algorithm, is quickly out of the reach of standard computers as the number of layers increases.

The main results of this paper can be summarized as follows.

At first, we consider materials with variable extinction coefficient and quarter-wavelength thicknesses. We found that, in this case, the optimal solution consist of two

sequences of cascade doublets, in which the doublets containing the non-dissipative material are positioned at the beginning of the coating.

Moreover, all the optimal solutions significantly outperform the reference solution consisting of QW layers made of silica and titania doped tantalum. The gain in terms of noise decreases as the extinction coefficient increases, for both categories of materials, and the optimal designs are robust with respect to the possible sources of uncertainty on the extinction coefficient. The spectral characteristics of transmittance satisfy the transmittance constraints in the entire band of interest.

Finally, we have shown that a further improvement in performance can be achieved using non-quarter wave layers.

Two words of caution on the method should be added. By its nature, the exhaustive search described above excludes periodic solutions containing half-wavelength unit cells made of three materials [31]. This problem, as already underlined above, involves an excessive computational burden and will be faced with heuristic techniques [13] in future work.

#### APPENDIX A - SEQUENCES COUNTING

The *multiplication principle* is used to count the total number of possible ways  $W$  in which an operation can be performed when the operation is performed in  $k$  steps, and each step can be done in a number of ways  $x_i$ . The answer is simple:

$$W = \prod_{i=1}^k x_i. \quad (\text{A22})$$

With this principle we are able to count the number of different coating structures  $\mathcal{N}_L$  with three layers. In accordance to the *multiplication principle* the first layer can be chosen in three ways. The second layer, in order to have no equal consecutive material, can be chosen in two ways. The same for the third layer, up to the last layer  $N_L$ . In view of eq. (A22) we have:

$$\mathcal{N}_L = 3 \cdot 2^{N_L-1}. \quad (\text{A23})$$

The same principle can be applied to counting the number of  $p_d$  different doublets. In this case, at any stage of layers sequence, we have  $p_d$  choices until the last doublet  $N_D$  is positioned on the substrate. We have the formula

$$\mathcal{N}_D = p_d^{N_D} \quad (\text{A24})$$

where, we note that for a doublet sequence  $N_L = 2N_D$ .

The formula (A24) also holds for the single layer search without the hypothesis of different adjacent layers:  $\mathcal{N}_L = p_l^{N_L}$ . In the Table IV, we have reported the normalized computation times of exhaustive searches when the number of doublets  $p_d$  varies. The computation times taken as a reference for doublet searches are those used in the paper (i.e.  $\sim 0.5h$  for  $p_d = 2$ ). We suppose that  $N_D = 18$  remain unchanged for all computed cases. In view of  $N_L = 2N_D$  the normalized computation time for the general single layer search is the square of doublet search.

#### ACKNOWLEDGMENTS

This work has been partially supported by INFN through the projects Virgo and Virgo-ET. The authors are grateful for the discussion and suggestions received from the Virgo Coating R&D Group and the Optics Working Group of the LIGO Scientific Collaboration.

$p_d$	scaled $\mathcal{N}_D$
4	262144.
5	$1.46 \times 10^7$
6	$3.87 \times 10^8$
7	$6.21 \times 10^9$
8	$6.87 \times 10^{10}$
9	$5.73 \times 10^{11}$
10	$3.81 \times 10^{12}$

TABLE IV. Estimated execution time normalized to the CPU time reported in the paper as a function  $p_d$  (number of doublets). We supposed  $N_D = 18$  is fixed in the computation.

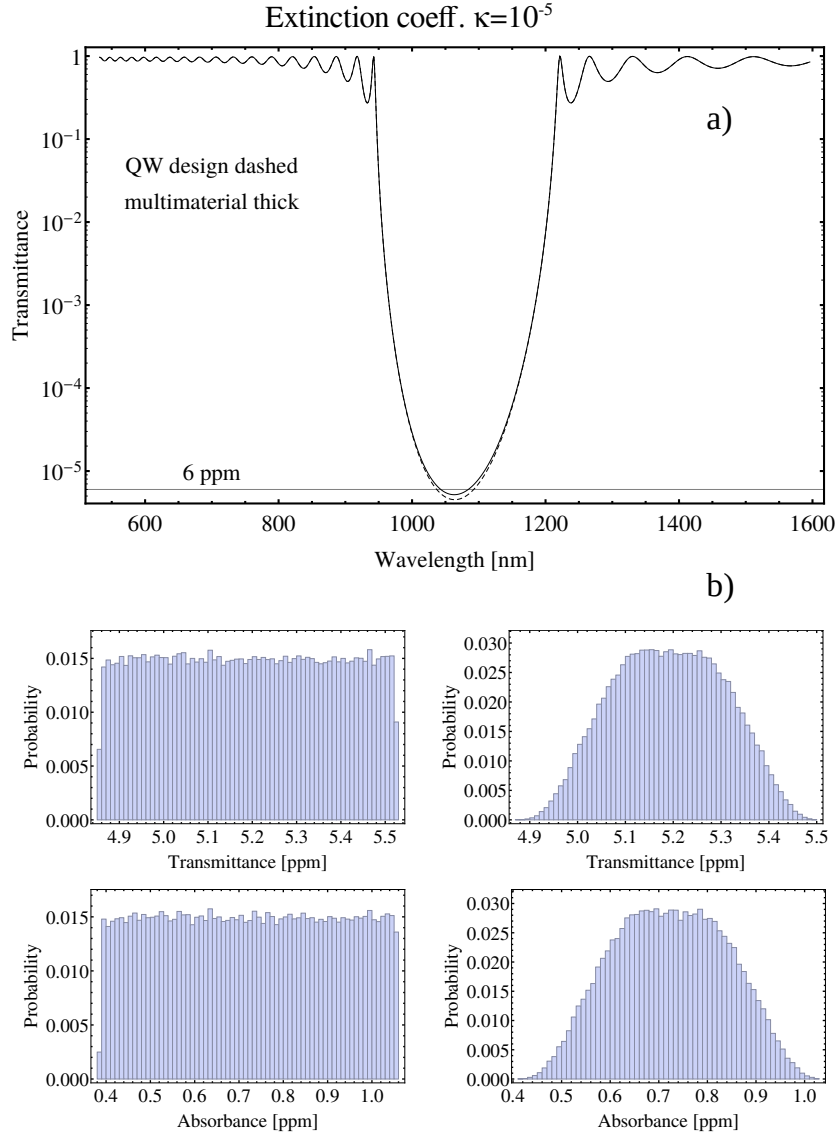


FIG. 6. In the part a) of the figure the frequency response of MA-type multicoating design with extinction coefficient  $\kappa = 10^{-5}$  is displayed as continuous curve, and is compared with the spectral response of QW reference design. In view of  $n_H \sim n_C$  the optical behaviour of the two coatings is very similar. In the part b) we show the distribution of transmittance and of absorbance assuming  $\kappa$  as a random variable. On the left b) part the extinction coefficient is supposed uniformly distributed in the range  $[0.5 \times 10^{-5}, 1.5 \times 10^{-5}]$  due to uncertainty in the measure. On the right b) part the extinction coefficient is supposed uniformly distributed in the range  $[0.5 \times 10^{-5}, 1.5 \times 10^{-5}]$  and variable for each dissipative layer as a random variable, this can possibly due to instabilities in deposition procedure.

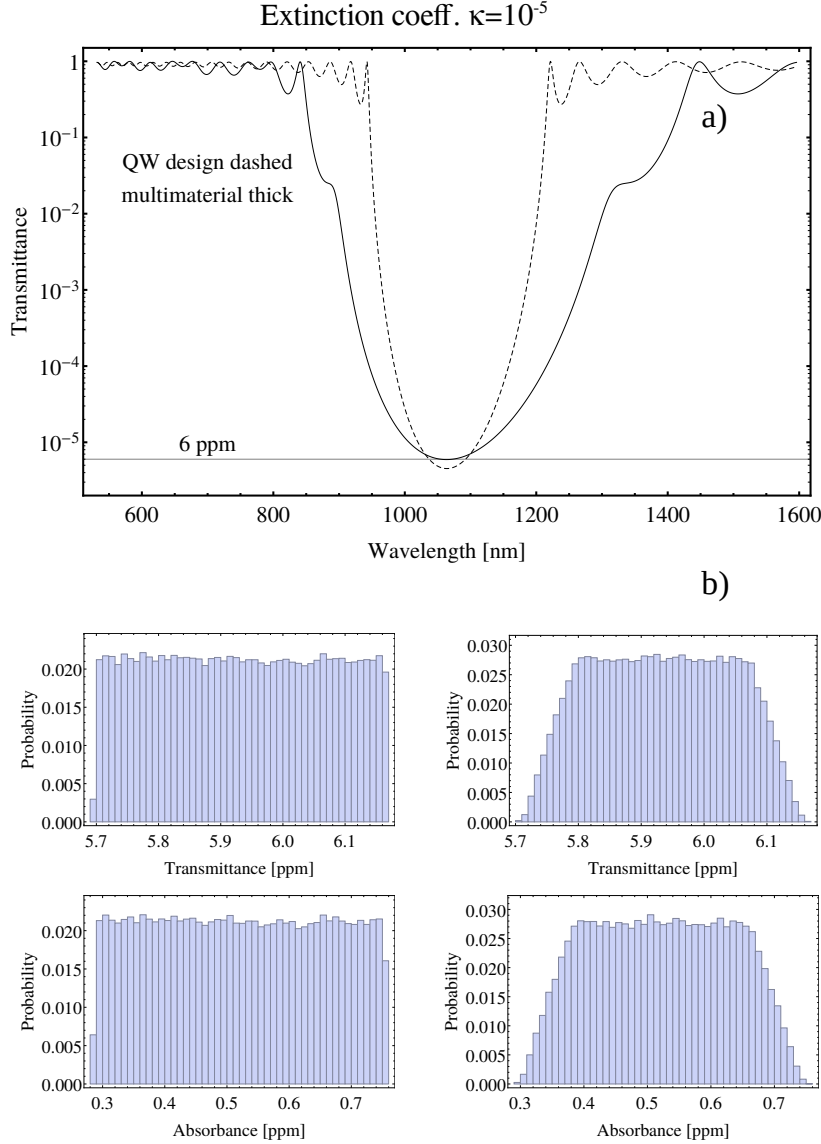


FIG. 7. In the part a) of the figure the frequency response of MB-type multicoating design with extinction coefficient  $\kappa = 10^{-5}$  is displayed as continuos curve, and is compared with the spectral response of QW reference design. In view of difference between  $n_H$  and  $n_C$  the optical behaviour is changed from QW reference design, in particular the transmission deep is wider than the QW reference deep and some secondary deep appear outside the QW reference design band. In the part b) we show in the distribution of transmittance and of absorbance assuming  $\kappa$  as a random variable. On the left b) part the extinction coefficient is supposed uniformly distributed in the range  $[0.5 \times 10^{-5}, 1.5 \times 10^{-5}]$  due to uncertainty in the measure. On the right b) part the extinction coefficient is supposed uniformly distributed in the range  $[0.5 \times 10^{-5}, 1.5 \times 10^{-5}]$  and variable for each dissipative layer as a random variable, this can possibly due to instabilities in deposition procedure.

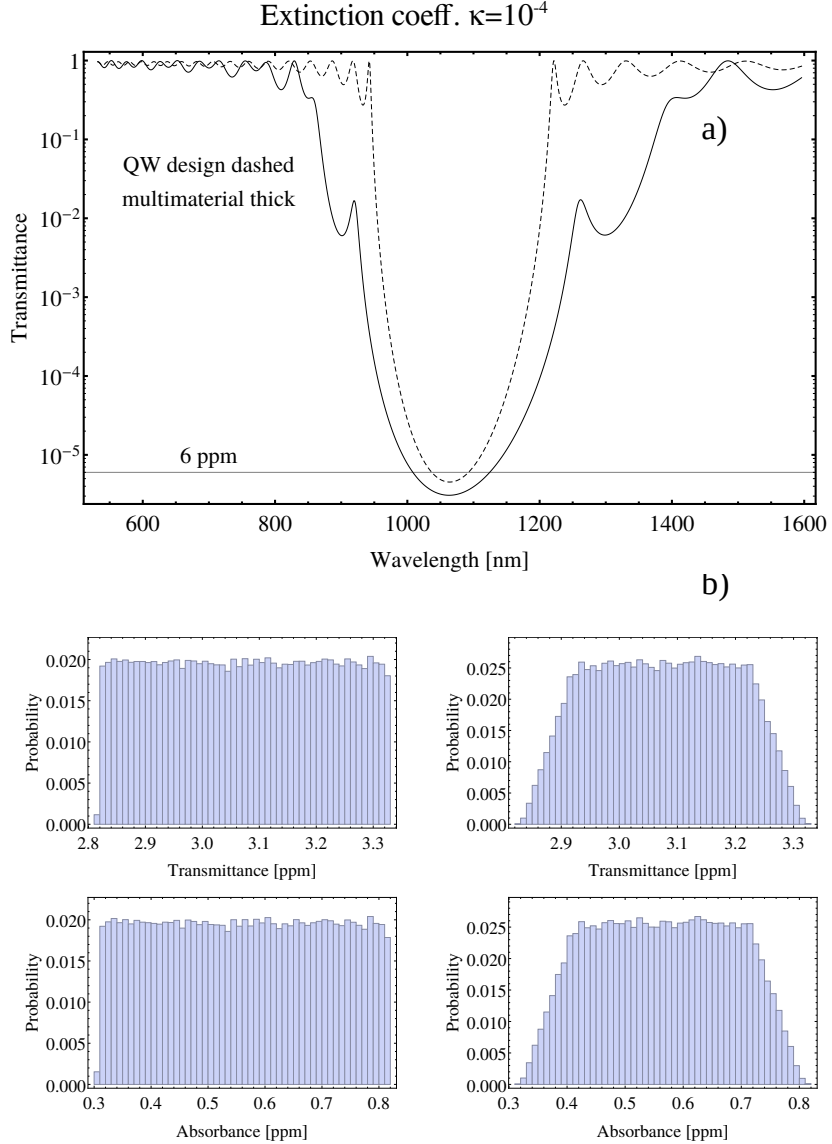


FIG. 8. In the part a) of the figure the frequency response of MB-type multicoating design with extinction coefficient  $\kappa = 10^{-4}$  is displayed as continuous curve, and is compared with the spectral response of QW reference design. In view of difference between  $n_H$  and  $n_C$  the optical behaviour is changed from QW reference design, in particular the transmission deep is wider than the QW reference deep and some secondary deep appear outside the QW reference design band. In the part b) we show the distribution of transmittance and of absorbance assuming  $\kappa$  as a random variable. On the left b) part the extinction coefficient is supposed uniformly distributed in the range  $[0.5 \times 10^{-5}, 1.5 \times 10^{-5}]$  due to uncertainty in the measure. On the right b) part the extinction coefficient is supposed uniformly distributed in the range  $[0.5 \times 10^{-5}, 1.5 \times 10^{-5}]$  and variable for each dissipative layer as a random variable, this can possibly due to instabilities in deposition procedure.

---

[1] web site <http://www.ligo.caltech.edu>

[2] web site <http://www.virgo.infn.it>

[3] Abernathy M R, Liu X and Metcalf T H 2018 *Materials Research* **21** e20170864

[4] Flaminio R, Franc J, Michel C, Morgado N, Pinard L and Sassolas B 2010 *Class. Quantum Grav.* **27** 084030

[5] Pinard L, Sassolas B, Flaminio R, Forest D, Lacoudre A, Michel C, Montorio J L and Morgado N 2011 *Optics Letters* **36** 1407–1409

[6] Harry G, Bodiya T P and DeSalvo R (eds) 2012 *Optical coatings and thermal noise in precision measurements* (Cambridge University Press)

[7] web site <https://gwcenter.icrr.u-tokyo.ac.jp/en/>

[8] Orfanidis S J *Electromagnetic Waves and Antennas* (web book <https://www.ece.rutgers.edu/~orfanidi/ewa/>)

[9] Pinard L, Michel C, Sassolas B, Balzarini L, Degallaix J, Dolique V, Flaminio R, Forest D, Granata M, Lagrange B, Straniero N, Teillon J and Cagnoli G 2017 *Applied Optics* **56** C11-C15

[10] Agresti J, Castaldi G, DeSalvo R, Galdi V, Pierro V and Pinto I M 2006 *Proc. of SPIE* **6286** 628608

[11] Villar A E, Black E D, DeSalvo R, Libbrecht K G, Michel C, Morgado N, Pinard L, Pinto I M, Pierro V, Galdi V, Principe M and Taurasi I 2010 *Phys. Rev. D* **81** 122001

[12] Kondratiev N M, Gurkovsky A G and Gorodetsky M L 2011 *Phys. Rev. D* **84** 022001

[13] Pierro V, Fiumara V, Chiadini F, Bobba F, Carapella G, Di Giorgio C, Durante O, Fittipaldi R, Mejuto Villa E, Neilson J, Principe M and Pinto I M 2019 *Optical Materials* **96** 109269

[14] Yam W, Gras S and Evans M 2015 *Phys. Rev. D* **91** 042002

[15] Steinlechner J and Martin I W 2016 *Phys. Rev. D* **93** 102001

[16] Pan H-W, Kuo L-C, Chang L-A, Chao S, Martin I W, Steinlechner J and Fletcher M 2018 *Phys. Rev. D* **98** 102001

[17] Steinlechner J, Martin I W, Hough J, Krüger C, Rowan S and Schnabel R 2015 *Phys. Rev. D* **91** 042001

[18] Ghédira K and Dubuisson B 2013 *Constraint Satisfaction Problems* (John Wiley and Sons, Inc. New York, NY)

[19] Knuth D E 1968 *The Art of Computer Programming* (Addison-Wesley)

[20] Dobrowolski J A 1976 *Thin Solid Films* **34** 313-321

[21] Pan H-W, Kuo L-C, Huang S-Y, Wu M-Y, Juang Y-H, Lee C-W, Cheng H-C, Wen T T and Chao S 2018 *Phys. Rev. D* **97** 022004.

[22] Steinlechner J, Krüger C, Martin I W, Bell A, Hough J, Kaufer H, Rowan S, Schnabel R and Steinlechner S 2017 *Phys. Rev. D* **96** 022007

[23] Birney R, Steinlechner J, Tornasi Z, MacFoy S, Vine D, Bell A S, Gibson D, Hough J, Rowan S, Sortais P, Sproules S, Tait S, Martin I W and Reid S 2018 *Phys. Rev. Lett.* **121** 191101

[24] Magnozzi M, Terreni S, Anghinolfi L, Uttiya S, Carnasciali M M, Gemme G, Neri M, Principe M, Pinto I, Kuo L-C, Chao S and Canepa M 2018 *Optical Materials* **75** 94–101

[25] Pan H-W, Wang S-J, Kuo L-C, Chao S, Principe M, Pinto I M and DeSalvo R 2014 *Optics Expr.* **22** 29847–29854

[26] F. Abelès 1950 *Le Journal de Physique et le Radium* **11** 307–310

[27] Allocca A, Gatto A, Tacca M, Day R A, Barsuglia M, Pillant G, Buy C and Vajente G 2015 *Phys. Rev. D* **92** 102002

[28] Martin I W, Chalkley E, Nawrodt R, Armandula H, Bassiri R, Comtet C, Fejer M M, Gretarsson A, Harry G, Heinert D, Hough J, MacLaren I, Michel C, Montorio J-L, Morgado N, Penn S, Reid S, Route R, Rowan S, Schwarz C, Seidel P, Vodel W and Woodcraft A L 2009 *Class. Quantum Grav.* **26** 155012

[29] The case  $N_L = 36$  needs a CPU Time equal to 6h on an Intel(R) Core(TM) i7-8700K CPU @ 3.70GHz

[30] <https://refractiveindex.info/>

[31] Pinto I M, Stacked-Triplet Ternary HR Coatings : Another Multimaterial Design Option, LIGO document G2000218-v1 (uploaded 20 Feb. 2020).